Electron-phonon interaction in the quantum Hall effect regime

F. Dietzel* and W. Dietsche
Max-Planck-Institut für Festkörperforschung, Heisenbergstraße 1, D70569 Stuttgart 80, Federal Republic of Germany

K. Ploog
Paul-Drude-Institut, Hausvogteiplatz 5-7, D10117 Berlin, Federal Republic of Germany
(Received 22 March 1993)

The absorption of ballistic phonons with frequencies in the 100-GHz range by a two-dimensional electron gas (2DEG) has been studied in a quantizing magnetic field. The 2DEG was formed at the interface of a $GaAs/Al_xGa_{1-x}As$ heterojunction. Acoustic phonons were created by heating the substrate locally with a focused laser beam. The phonons traveled ballistically through the crystal and were partially absorbed by the 2DEG. This led to a transfer of momentum into the 2DEG (phonon-drag effect) resulting in phonon-induced voltages and currents. These quantities gave detailed information about the interaction between acoustic phonons and the 2DEG as a function of both the incident angle of the absorbed phonons and the magnetic field. We observed that the dependence of the phonon-drag signal on the angles of incidence was neither affected by the magnetic field nor by the phonon spectrum. The absolute intensity of the phonon-drag signal, however, oscillated in phase with the Shubnikov–de Haas oscillations. These results could be explained with a simple microscopic theory of the electron-phonon interaction together with a macroscopic model for the response of the 2DEG on the absorption of ballistic phonons.

I. INTRODUCTION

The interaction between ballistic phonons and a two-dimensional electron gas (2DEG) has been the subject of intense research over the last decade.[1–8] Due to the reduced dimensionality of the 2DEG the interaction with the three-dimensional phonons differs in a substantial way from the one with a three-dimensional electron gas.[2,8] Another interesting aspect is the large wave vector of the phonons which is comparable with the Fermi wave vector of the 2DEG. This allows the probing of the 2DEG in the momentum space in contrast to optical measurements which are sensitive to energy. On the other hand, the energy relaxation in electronic devices is determined by the electron-phonon interaction. Thus, its understanding is also important from a technological point of view.

Even more interesting is the case of the electron-phonon interaction (EPI) in a strong magnetic field B. The occurence of the quantum Hall effect (QHE) at low temperatures indicates the drastic change of the 2DEG. The EPI in a strong magnetic field has been studied theoretically.[8,9] Experimental data are available from thermal conductivity measurements,[6] from thermoelectric data,[10,11] and from heat-pulse measurements.[3,4]

In this paper we report on our recent experimental results on the EPI in a strong magnetic field. All measurements and analyses were made for the $GaAs/Al_xGa_{1-x}As$ heterostructure system. We used the phonon-drag imaging technique[5] in order to study the EPI in a quantizing magnetic field as a function of the phonon modes and their respective angle of incidence. It will be shown that the EPI depends on the density of states of the electrons and on a cutoff caused by form factors due to both the Landau radius and the thickness of the 2DEG. We will also show that in experiments in high magnetic fields the design of the sample geometry plays a crucial role in the correct interpretation of the results. This is due to the nontrivial current and potential distributions in the QHE samples.

This paper will be organized as follows: in Sec. II we develop the theoretical description of our experimental situation. In Sec. III we describe the experimental setup and our measurement technique. In Sec. IV we will report on our data of the imaging experiments while Sec. V is devoted to the magnetic-field dependence of EPI and the discussion of these results in the framework of the theory developed in Sec. II.

II. THEORETICAL BACKGROUND

The 2DEG is a thin layer of electrons in the GaAs near the interface of the heterostructure. We choose the coordinate system in such a way that the 2DEG lays in the x-y plane. A potential $V(z)$ causes the localization of the electrons in the z direction. The electronic states in zero magnetic field are given by

$$\Psi_{i,k_\parallel}(x,y,z) = e^{i\mathbf{k}_\parallel\cdot\mathbf{r}_\parallel}\Phi_i(z)\frac{1}{\sqrt{L_xL_y}} \quad , \tag{1}$$

where $\mathbf{r}_\parallel$ and $\mathbf{k}_\parallel$ are the cordinates in the x-y plane and the momenta in the two-dimensional $\mathbf{k}$ space, respectively. $\Phi_0(z)$ is the wave function of the lowest subband determined by $V(z)$, and L_xL_y is the area of the 2DEG in the x-y plane. Higher subbands are not considered because they were not occupied in the samples studied in this work.

The rate $(\tau_{e\text{-}p}^{\beta})^{-1}$ with which the 2DEG absorbs a phonon in the state β with the energy $\hbar\omega_\beta$ can be calculated by first-order perturbation theory to be

$$(\tau_{e\text{-}p}^{\beta})^{-1} = \frac{2\pi}{\hbar} \sum_{\substack{i,f \\ E_i = E_f - \hbar\omega_\beta}} |M^\beta|^2 \; |\langle i \mid e^{i\mathbf{q}_s \cdot \mathbf{r}} \mid f\rangle|^2 \times f(E_i)[1 - f(E_f)] \; . \quad (2)$$

This rate depends on the probability that the initial and the final electron states are occupied and empty, respectively, as expressed by the Fermi function f, which depends on the electron temperature T_E and the chemical potential E_μ. The term $M^\beta \langle i \mid e^{i\mathbf{q}_s \cdot \mathbf{r}} \mid f\rangle$ is the matrix element of the EPI. To get the explicit form of M^β one must know the precise mechanism of the EPI. The second part of the matrix element contains an integral over the wave functions in the initial and the final states. The matrix element is in general reduced by screening which will not be included in our theoretical description.

Before discussing Eq. (2) further we will treat the matrix element of the EPI in more detail. Acoustical phonons are absorbed by the 2DEG either by the deformation potential or by the piezoelectric interaction.[12]

Formally these matrix elements can be written as[12,9]

$$M_{\text{def}}^{\beta} = \left(\frac{\hbar}{2\rho_K \omega_\beta V}\right)^{\frac{1}{2}} i \, \Xi_d \, \mathbf{q}_s \mathbf{e}_\beta \; , \quad (3)$$

$$M_{\text{piezo}}^{\beta} = \left(\frac{\hbar}{2\rho_K \omega_\beta V}\right)^{\frac{1}{2}} \frac{2h_{14}e}{q_s^2} \times (q_x q_y e_{z,\beta} + q_y q_z e_{x,\beta} + q_z q_x e_{y,\beta}). \quad (4)$$

Here ρ_K is the density of the crystal, V its volume, e the elementary charge, $\mathbf{q}_s$ and $\mathbf{e}_\beta$ are the wave vector and unit vector of the mechanical polarization of the phonons, and Ξ_d and h_{14} are the constants of the deformation potential and the piezoelectric interaction, respectively.

If the wave functions from Eq. (1) are put in $\langle i|e^{i\mathbf{q}_s \cdot \mathbf{r}}|f\rangle$ then the conservation rules for the wave-vector momenta are obtained,

$$\langle i \mid e^{i\mathbf{q}_s \cdot \mathbf{r}} \mid f\rangle = F(q_z) \; \delta_{\mathbf{k}_i + \mathbf{q}_\parallel, \mathbf{k}_f} \; . \quad (5)$$

$\mathbf{k}_i$ and $\mathbf{k}_f$ denote the wave vectors of the initial and final states, respectively, $\mathbf{q}_\parallel$ is the momentum component of the absorbed phonons lying in the plane of the 2DEG, and $|F(q_z)|^2$ is the form factor

$$|F(q_z)|^2 = \frac{1}{(1 + q_z^2 a_0^2)^3} \; , \quad (6)$$

where a_0 is a measure for the extension of the 2DEG in the z direction. The form factor is at most 1 and vanishes if

$$q_z a_0 \gg 1 \; , \quad (7)$$

which reflects just the uncertainty relation principle. The Kronecker symbol in Eq. (5) assures the momentum conservation within the x-y plane,

$$\hbar\mathbf{k}_f = \hbar\mathbf{k}_i + \hbar\mathbf{q}_\parallel \; . \quad (8)$$

The initial and final states $\hbar\mathbf{k}_i$ and $\hbar\mathbf{k}_f$ differ by at most $2\hbar k_F$

$$\hbar \, |\mathbf{k}_i - \mathbf{k}_f| \leq \hbar 2k_F \; . \quad (9)$$

Thus there are two mechanisms which limit the absorption of large wave-vector phonons as expressed by the two Eqs. (7) and (9).

If a quantizing magnetic field is applied to the 2DEG then the wave functions entering Eq. (2) are replaced by

$$\Psi_{0,n,k}(x,y,z) = u_n(x - X) e^{iky} \Phi_0(z) \frac{1}{\sqrt{L_y}}, \quad (10)$$

where u is the harmonic-oscillator function with frequency $\omega_c = eB/m^*$ located at the coordinate X, given by

$$X = l_B^2 k. \quad (11)$$

$l_B = \sqrt{\hbar/(eB)}$ is the magnetic length. The field dependence of the subband wave functions can be neglected in first order.

The first term of the matrix element M^β is not changed by the magnetic field. The second one becomes

$$\langle i \mid e^{i\mathbf{q}_s \cdot \mathbf{r}} \mid f\rangle = - \left(\frac{2^n n!}{2^{n'} n'!}\right)^{\frac{1}{2}} e^{-\frac{\zeta^2}{4}} \zeta^{2n'-2n} \times L_n^{n'-n}\left(\frac{\zeta^2}{2}\right) F(q_z) \delta_{k_i + q_y, k_f}. \quad (12)$$

Here $\zeta = q_\parallel l_B$ and $L_n^{n'-n}$ is the generalized Laguerre polynomial. The momentum conservation in the y direction is contained in Eq. (12) as

$$k_i + q_y = k_f. \quad (13)$$

It also determines the distance ΔX between the center coordinates of the initial and final states. One obtains with Eq. (11)

$$\Delta X = q_y l_B^2 \; . \quad (14)$$

Thus, the transfer of momentum $\hbar q_y$ in the y direction is equivalent to the movement of an elementary charge by $q_y l_B^2$ in the x direction. Whether there is any phonon absorption at all will depend on the overlap of the wave functions in the x direction which is characterized by l_B. The factor $\exp(-\zeta^2/4)$ in Eq. (12) describes this. The condition on $q_\parallel$ from Eq. (9) is therefore modified by the presence of a magnetic field by

$$q_\parallel l_B \gg 1. \quad (15)$$

Thus whether there is a magnetic field or not the EPI has always the character of a low-pass filter. At $B = 0$ T ($B \neq 0$ T) only phonons with $q_z a_0 < 1$ and $q_\parallel < 2k_F$ ($q_\parallel l_B < 1$) are absorbed. All phonon states are within a cylinder with the height of $1/a_0$ and a radius $r = 2k_F$ for $B = 0$ T ($r = 1/l_B$ for $B \neq 0$ T).

Assuming a value of 10 nm for a_0 leads to a perpendicular cutoff at $k_z = 10^6$ cm^{-1}. The $2k_F$ cutoff (with $n_e = 3.76 \times 10^{11}$ cm^{-2} as the charge density) will occur at

$k_{\|} = 3 \times 10^6$ cm^{-1}. The in-plane cutoff in the case of the magnetic field is $k_{\|} = 3.9\sqrt{B\ (\mathrm{T})}10^5$ cm^{-1}. In real space the situation is more complicated because of the phonon focusing effects. The volume of interacting phonons in real space has a very complicated shape[13] instead of the simple cylinder in momentum space.

In a ballistic phonon experiment the momenta of the absorbed phonons is transfered to the electrons acting as a "phonon force" on the electrons. This leads to measureable phonon-drag voltages and currents. The momentum per unit time and electron $\mathbf{F}^p$ (phonon force) that is transfered from the phonons to the 2DEG is given by

$$\mathbf{F}^p = \sum_\beta \frac{I(\beta)}{v_g(\beta)}\, \hbar \mathbf{q}_{\|}(\beta) \frac{(\tau_{e\text{-}p}^{\beta})^{-1}}{N_e}, \tag{16}$$

where $I(\beta)$ specifies the flux of the ballistic phonons indexed by β, $v_g(\beta)$ is their group velocity, N_e is the number of electrons in the 2DEG, and $\mathbf{q}_{\|}(\beta)$ is the component of the phonon wave vector in the plane of the 2DEG.

For the interpretation of the experimental result a relation between the microscopic momentum transfer rate $\mathbf{F}^p$ given by Eq. (16) and the resulting macroscopic electric current densities $\mathbf{j}$ and fields $\mathbf{E}$ is needed. Several models have been developed to interpret thermoelectric[14–17] and ballistic phonon data.[17] We use a very simple description which is based on a recent publication by Efros *et al.*[18] Our essential assumption is that the phonon force exerted by the absorbed phonons induces currents in the same way as if they were caused by electric fields,

$$\mathbf{j} = \hat{\sigma}\left(\mathbf{E} - \frac{\mathbf{F}^p}{e}\right), \tag{17}$$

$\hat{\sigma}$ is the conductivity tensor. This tensor equation can be reduced by using the experimental boundary conditions $E_x = 0$ and $j_y = 0$. Since $F_x^p \approx F_y^p$ and $\sigma_{xx} \ll \sigma_{xy}$ we get the result

$$E_y \approx \frac{\sigma_{xy}}{\sigma_{xx} e} F_x^p \tag{18}$$

and

$$j_x \approx \frac{\sigma_{xy}^2}{\sigma_{xx} e} F_x^p\,. \tag{19}$$

Dividing these two equations by each other leads to the Hall resistance

$$\frac{E_y}{j_x} \approx \frac{1}{\sigma_{xy}}. \tag{20}$$

The first of these three equations describes a phonon-induced Hall voltage while the second one corresponds to the current. The components of the conductivity tensor are available from standard electric transport measurements. Thus the phonon momentum-transfer rate to the 2DEG can be calculated either from a measurement of the phonon-drag induced current or from the phonon-Hall voltage. In all of our considerations we neglect the phonon absorption by edge states, which seems to cause resistivity changes[19] but no phonon-drag effect.

III. EXPERIMENTAL TECHNIQUES

The samples were standard GaAs/$Al_xGa_{1-x}As$ heterostructures grown on (001)-oriented GaAs substrates of about 350-μm thickness. The samples had to be transparent for ballistic phonons in the 100-GHz range, therefore they had to be undoped by chromium.[20] We restricted ourselves to the use of samples without any parallel conducting channel in the heterostructure even under continous illumination with laser light[21] although other samples showed a qualitatively similar behavior. We did not find a dependence of our results on mobility and carrier density. The sample with which the data of Sec. IV were obtained had a mobility μ at 4.2 K of 1.6×10^6 cm^2/V sec while the carrier density n_e was 3.76×10^{11} cm^{-2}.

The 2DEG was structured by wet etching. Ohmic contacts were made by alloying AuGeNi. Onto the substrate side opposite to the 2DEG an aluminum film of 2000-Å thickness was evaporated. The experimental setup is sketched in the top of Fig. 1. It is similar to the one used by Karl *et al.*[5] who utilized the phonon imaging technique.[22] The sample was placed into a ^{4}He cryostat operating at 1.1 K and was surrounded by a superconducting solenoid capable of creating fields up to 12 T. Optical access to the sample was provided by a window

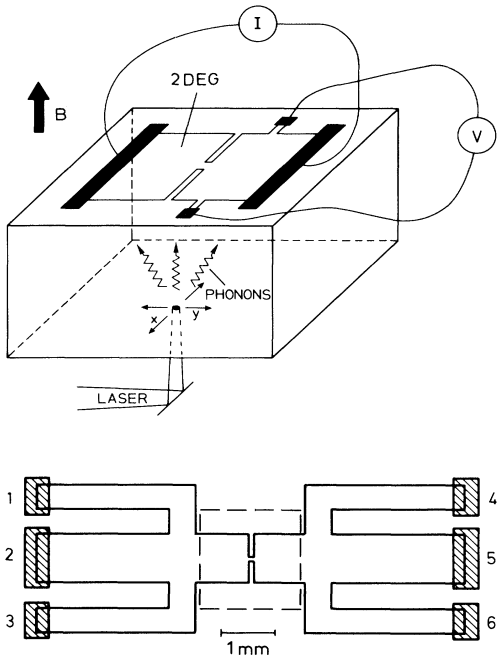

FIG. 1. Top: Schematic view of the experimental setup. The laser heats up the Al film on the bottom of the crystal and phonons with frequencies far above those of the thermal equilibrium are emitted. Phonons absorbed in the narrow bridge in the center of the 2DEG structure cause a phonon-drag signal if they have a momentum component in the bridge direction. The laser focus is scanned over the surface and both the phonon-induced currents and the perpendicular Hall voltage are being recorded as a function of laser position. Bottom: Correct outline of the 2DEG structure used in our experiments.

at the bottom of the cryostat. Through this window an argon laser beam ($\lambda = 514.5$ nm) was focused on the Al film on the bottom of the substrate. The diameter of the focus was about 10 μm. The absorbed laser light raised the film temperature to typically 15 K (Ref. 23) depending on the absorbed laser power P_L which was estimated to vary between 0.7 mW and 12.5 mW. High-frequency phonons were emitted by the heated spot which traveled ballistically to the top side where they were partially absorbed by the 2DEG.

Only the narrow bridge with an area of 50 μm$\times$50 μm acted as the sensitive area for the ballistic phonon-drag signal. In the larger contact areas the locally induced electric fields canceled each other or were screened due to the finite conductivity of the 2DEG. Both the phonon-induced current through the source and drain contacts and the phonon-induced Hall voltage was measured using the lock-in technique operating at about 500 Hz. No external current was applied to the device. The signal was recorded by a computer which also controlled the position of the laser focus by two galvanometer-driven mirrors. In order to obtain an "image" of the phonon-drag signal the signal was displayed on a monitor as gray tone while the laser focus was raster scanned.

The actual shape of the 2DEG structure is shown in the bottom of Fig. 1. Not all of the contacts were shown in the top panel. The line connecting the contacts 3 and 5 is the [110] direction. The structure had a shape related to the commonly used Hall bars but the voltage probes 1, 2, 4, and 6 are moved away from the center. Both the longitudinal magnetoresistance R_{xx} and the Hall resistance R_{xy} were measured in addition to the phonon-drag measurements. The reason why all contacts were moved more than 3.5 mm away from the sensitive area of the 2DEG was to keep them at the bath temperature during the phonon experiment. Otherwise spurious voltages were created by the temperature difference of the contacts due to thermoelectric effects. This effect was responsible for unexplained phenomena in previously published images[5] as was shown by Ref. 24.

In a magnetic field the situation was more complicated because temperature gradients perpendicular to the contacts caused a voltage, called the Nernst-Ettingshausen effect, even if the contacts were at the same temperature. We will show in the next section how the phonon-drag effect and the Nernst-Ettingshausen effect could be separated.

IV. PHONON-DRAG IMAGING

In the experiments we took images of the phonon-drag voltage at different magnetic fields and laser powers. This was done initially by using the contacts 3 and 5 of Fig. 1. In Fig. 2 (top) the result can be seen for $B = 0$ T and an absorbed laser power of about 3 mW.

An average gray tone indicated a phonon-drag voltage of 0 V. A light (dark) tone corresponds to a positive (negative) signal. The voltages were always less than 500 nV. The anisotropy of the image was a result of the anisotropic ballistic phonon flux through the crystal (phonon focusing[22]). The sharp ridges were due to

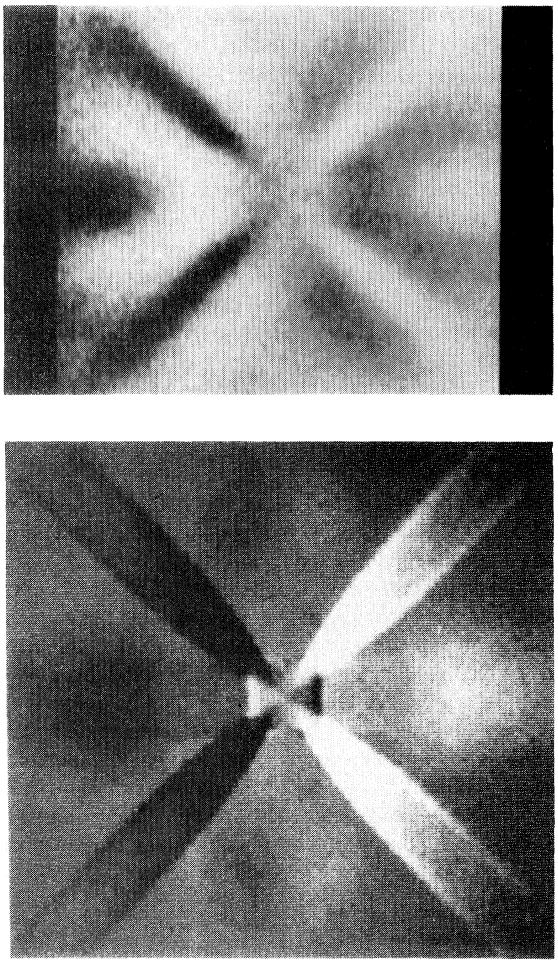

FIG. 2. Top: Image of the phonon-drag voltage in zero magnetic field measured using the contacts 2/5 of Fig. 1. An average gray tone corresponds to zero signal. Positive and negative signals are represented as dark and bright shades, respectively. The sharp diagonal ridges are due to FTA phonons while the round areas in the left and right are caused by LA phonons traveling near the $\langle 111 \rangle$ directions. Bottom: Phonon-drag image calculated using the piezoelectric interaction.

fast tranverse (FTA) phonons propagating in or near the $\{100\}$ planes. The two larger round areas were due to longitudinal phonons which were focused near the $\langle 111 \rangle$ directions. The sign reversal (left/right) was due to the different directions of the phonon force in the two halves of the image.

The observation of the focusing pattern proved that ballistic phonons contributed to the observed image only and that they were detected only by the bridge in the 2DEG structure. This image was similar to the experimental findings of Karl *et al.*,[5] except that thermal voltages caused by the contacts were now absent. Thus, our image was in better agreement with the one predicted theoretically[5,25] shown as Fig. 2 (bottom). This image was calculated assuming piezoelectric interaction only.

By changing the laser power the phonon spectrum of the ballistic phonons impinging on the 2DEG was

changed. Although we observed an overall rise in the phonon-drag voltage there was no systematic change in the shape of the pattern. In particular, there was no transition to the image expected from deformation-potential coupling which should dominate at high phonon energies and no indication of the $2k_F$ cutoff in the images.

We attribute this negative result to the low-pass behavior of the EPI: Even if the phonon intensity was dramatically increased, only a very small fraction at the low-frequency end of the Planck spectrum was absorbed; see Sec. II. In the spectroscopy results of Lega *et al.*,[7] however, the cutoff was observed. Possibly, the thickness parameter a_0 of their 2DEG sample was smaller than ours.

The images changed drastically after high magnetic fields had been turned on. In addition, there was not just one type of pattern but we found that, depending on the filling factor, four qualitatively different situations had to be distinguished.

(i) If the Fermi energy was in the region of localized states, i.e., if we were in the quantum Hall regime, then we did not observe any signal at all.

(ii) If the Fermi energy was in the lower half of the extended states region then we observed strong signals leading to very diffuse images like the one shown in Fig. 3, which were not of ballistic origin. Only a weak part of this image was caused by ballistic phonons. Much more striking were the large diffuse areas of positive and negative voltages in the upper and lower part of the image, respectively. Thus this type of signal seems to be rotated with respect to the axis connecting the contacts.

(iii) If the Fermi energy was in the upper half of the extended states region then the image was qualitatively the same, but the voltages leading to the diffuse parts of the images reversed sign. Thus the image was dark in the upper part and bright in the lower one. The faint ballistic part in the image remained unchanged.

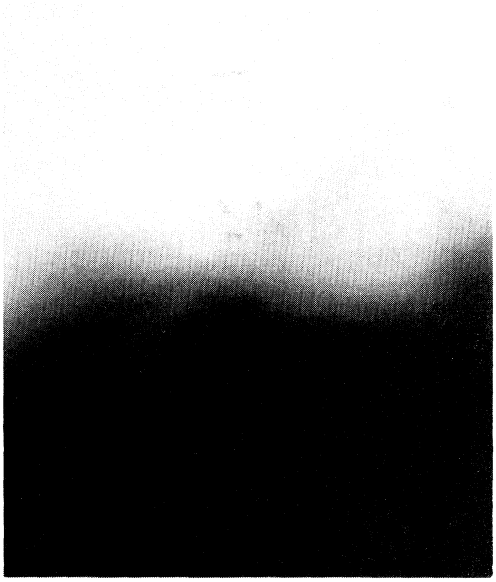

FIG. 3. Image of the phonon-induced voltages across the contacts 2/3 in a magnetic field of about 4.5 T. The Fermi energy is in the lower half of a Landau level. The large diffuse areas (bright at top, dark at bottom) are due to the Nernst-Ettinghausen effect. A ballistic phonon-drag image is superimposed on this image but is hardly visible in the reproduction.

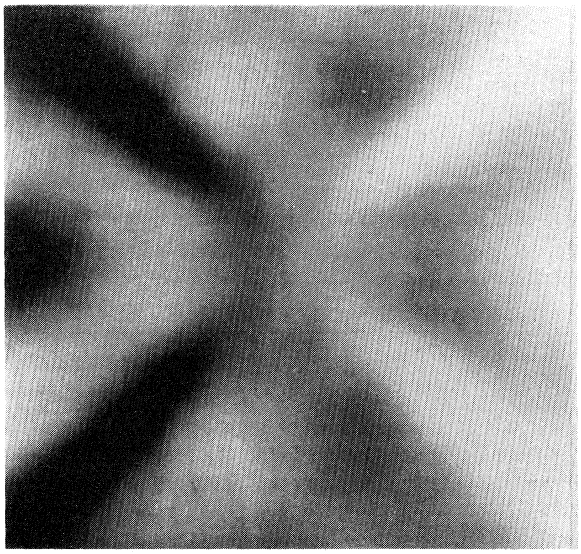

FIG. 4. Ballistic phonon-drag image taken at $B \approx 12$ T by measuring the voltages across the contacts 2/3. At this field the Nernst-Ettinghausen effect was zero because the Fermi energy was in the center of a Landau level. Note that the image is not rotated with respect to the image of Fig. 1.

(iv) Consequently, the magnetic field could be set such that the diffuse part of the image vanished. In this situation the ballistic part only became visible. Now the Fermi energy was approximately in the center of the extended states region. An image taken under this condition is shown as Fig. 4 for a magnetic field of about 12 T.

We attribute the diffuse signal to thermal voltages caused by a temperature gradient across the sample. The reason was the heating of the 2DEG by the very intense beam of highly focused phonons along the [001] direction. This gradient caused a transverse thermal voltage (Nernst-Ettingshausen effect) in magnetic fields as mentioned in Sec. III. This interpretation was verified by focusing the laser beam to a position where no ballistic phonon signal was observed and by recording the voltage as function of the magnetic field (Fig. 5). Most significant are the oscillations of the signal around zero voltage. This behavior was qualitatively the same as that of S_{xy} observed in Ref. 10. Another feature of this voltage was that it changed sign on reversing the magnetic-field direction. When adding two images at two fields $\pm B$ a ballistic phonon-drag image like the one in Fig. 4 was obtained. Thus the ballistic images were not affected by the direction of the magnetic field.

The ballistic phonon-drag images have two interesting features which should be discussed here. One of them was surprising at first.

From Fig. 4 it seemed as if the electric field induced by the force Eq. (16) of the absorbed phonon momenta points into the same direction as the momenta them-

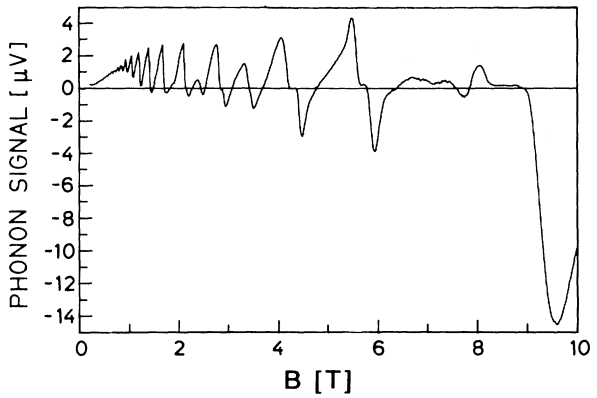

FIG. 5. Intensity of the Nernst-Ettinghausen signal as a function of the magnetic field. The oscillatory behavior around zero is typical of the effect.

selves. One would have expected that the image in Fig. 4 was rotated with respect to the one of Fig. 2 (top) by 90° due to the Lorentz force. However, we overlooked initially that the image in Fig. 4 was due to the phonon-induced current even if it was measured with a high impedance voltmeter. Actually, the internal fields *were rotated.* However, the spatial current and electric-field distribution were always deformed near the contacts in QHE samples in such a way that the phonon Hall voltage was measured in a two-point geometry. Thus, the internal electric fields did not point in the direction defined by the contacts. On the other hand, if an ampere meter was connected to the contacts 2/3 (or if they were shorted) and if the phonon Hall voltage at the contacts 4/6 was recorded then the internal potential distribution was forced to be homogeneous in the regions of both the voltage probes and the imaging range. In this case we found that both patterns, the one of Fig. 3 and the one of Fig. 4, were rotated by 90°. Thus the phonon-drag-induced electric field was now indeed perpendicular to the phonon momenta as expected from Eq. (18). The Nernst-Ettinghausen voltage, on the other hand, pointed in the direction of the temperature gradient.

The second interesting feature was that the shape of the phonon-drag image was not dependent on the magnetic field. Its intensity varied dramatically as will be discussed in Sec. V but the image pattern remained essentially the same at all magnetic fields. In view of the theory of Sec. II this insensitivity to the magnetic field was expected because the images were mainly determined by the term M^{β} of the matrix element which is not dependent on **B**. The form factors stemming from the other term $\langle i \mid e^{i\mathbf{q}_s\cdot\mathbf{r}} \mid f\rangle$ were not readily observable because the form factor cutoff in the z direction is the same with and without field while the $2k_F$ cutoff at zero field and the magnetic-length cutoff in high fields are of the same order of magnitude.

V. MAGNETIC-FIELD DEPENDENCE OF THE PHONON DRAG

For the quantitative analysis of the dependence of the phonon-drag voltage on the magnetic field both the phonon-drag-induced current through contacts 2/5 and the corresponding phonon Hall voltage at contacts 4/6 were measured. Separation of the ballistic part of the image from the diffusive background was made easy by the sharp focusing features of the ballistic pattern. The laser was first focused onto the intense FTA ridge of the ballistic image and then onto two points next to this ridge. From the voltage measurement at the latter two points the background at the first one was calculated and then subtracted out. The resulting voltages and currents are plotted in Fig. 6 (top panel) as a function of the magnetic field. The phonons which were studied in this way traveled along the [012] crystallographic direction.

It is immediately obvious from Fig. 6 (top) that the signal followed roughly the longitudinal resistance in a Shubnikov–de Haas measurement. In particular, one sees that the phonon signal disappears in regions where the

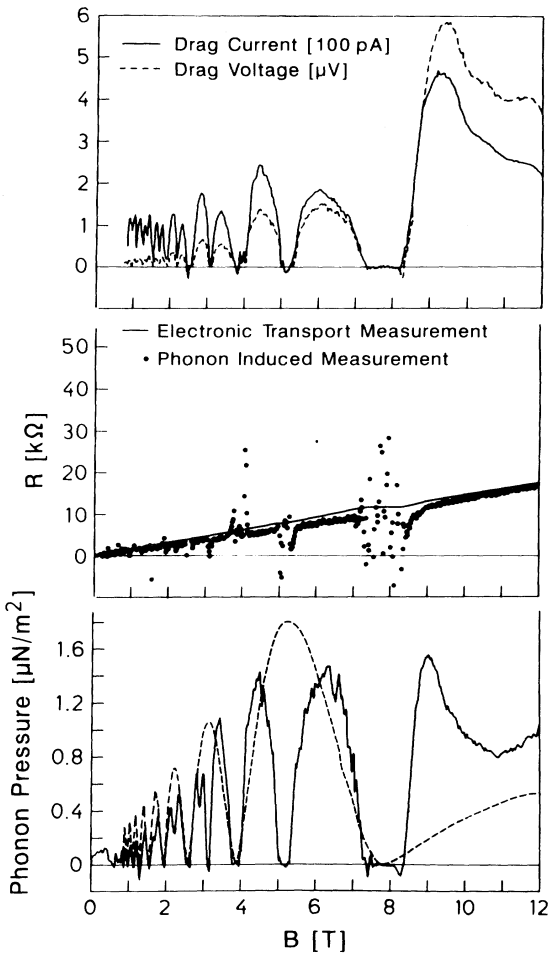

FIG. 6. Top: Ballistic phonon-drag Hall voltages and currents taken at a point on the FTA ridge which corresponds to the [012] direction. Center: Comparison of the Hall resistance calculated from the phonon-induced currents and voltages with the one obtained from conventional transport measurements. Bottom: Phonon force acting on the 2DEG (solid line). The dashed curve is the result of a calculation based on a simple model. The deviations are mainly due to the deficiencies in the model density of states.

conductivity vanished, i.e., in the regions of the QHE. The maximum amplitude of the signal in the other regions increased strongly with magnetic field. We will show that this behavior is due to the increase of the density of states at the Fermi edge.

The model which has been described in Sec. II was used to analyze the experimental data. In the region of the QHE no analysis was possible because both σ_{xx} and $\mathbf{F}^p$ tend to be zero. We can say, however, from our data that there was no phonon-drag signal as long as $\sigma_{xx} = 0$, i.e., as long as the Fermi energy was in the range of the localized states.

In the other regions a first test of the model was provided by dividing the measured phonon-drag Hall voltage by the phonon-drag current. According to Eqs. (18) and (19) this should just give the Hall resistance. In Fig. 6 (center) the result is shown together with the Hall resistance measured by standard transport measurement. In the QHE range the result was ill defined, of course, but otherwise the phonon Hall resistance agreed well with the transport Hall resistance. Using Eq. (18) one can now calculate the phonon force $\mathbf{F}^p$ because σ_{xx} is known from the transport measurements. The result is shown as the solid line in Fig. 6 (bottom). Note that the phonon force can be given in absolute units (μN/m^2).

In order to compare this experimental result with the theory we calculated the phonon force using the model presented in Sec. II. According to Eq. (16) one needs both the theoretical values for $(\tau^{\beta}_{e\text{-}p})^{-1}$ and the phonon spectrum $I(\beta)$. To get the first quantity we assumed that the scattering is quasielastic, i.e., that phonon energies are small compared to the width of the Landau levels. Thus, it was possible to calculate the intra-Landau level transitions which were not contained in the model of Sec. II. Now Eq. (2) can be simplified using Eq. (12) to

$$(\tau^{\beta}_{e\text{-}p})^{-1}_{B\neq 0} = \frac{2\pi\omega_\beta}{1-\exp(-\hbar\omega_\beta/k_B T_E)} \pi l_B^2 \, L_x L_y \, D(E_\mu, B)^2 \times |M^\beta|^2 \, |\langle i \mid e^{i\mathbf{q}_s\cdot\mathbf{r}} \mid f\rangle|^2_{k_i+q_y=k_f} \quad , \tag{21}$$

where $D(E_\mu, B)$ is the density of electronic states (DOS) at the Fermi level. We take the DOS suggested by Ando[26]

$$D_n(E,B) = \sqrt{\frac{2}{\pi\Gamma(B)^2}} \frac{1}{\pi l_B^2} \exp\left(-\frac{2[E-E(0,n)]^2}{\Gamma(B)^2}\right), \tag{22}$$

where $\Gamma(B) \sim \sqrt{B\ (\mathrm{T})}$ is the width of the impurity-broadened Landau levels. This DOS neglects both the spin splitting and the existence of the localized states.

The phonon flux $I(q)$ of these phonons was described by a Planck spectrum determined by the phonon temperature T_P. The phonon temperature followed from the power dissipated in the heater film. The model of Ref. 23 was used for an estimate and we found for our experimental situation $T_p = 10\ \mathrm{K} \times [2.83 P_L\ (\mathrm{mW})]^{1/4}$. At a typical absorbed power of 3 mW corresponding to a power density of 38 W/mm^2 one obtained a T_P of 17 K.

For the numerical calculation the following parameters were used: $T_E = 1.64$ K, $\rho_K = 5.3$ g/cm^3, $v_{FT} = 3.36 \times 10^5$ cm/sec,[27] $h_{14}e = 1.45 \times 10^{10}$ meV/m,[27] $a_0 = 10$ nm, $\Gamma = 0.6$ meV $\sqrt{B\ (\mathrm{T})}$, and $N_e = 3.76 \times 10^{11}$ cm^{-2}. The chemical potential was determined by $N_e = \int_0^\infty dE f(E_\mu, T_E) D(E,B)$. The calculated result is shown as a dashed line in Fig. 6 (bottom). Its intensity was approximately fitted to the experimental data.

The two main discrepancies in the magnetic-field dependence between theory and experiment were expected. One was the absence of the spin splitting in the theoretical trace which was not contained in the theoretical DOS. Thus only every other minimum in the experimental trace was reproduced by the theory. The other one was due to the existence of the localized states which were not contained in the model DOS. Thus the wide regions of zero phonon drag in the QHE regions could also not be reproduced.

On the other hand, the amplitude of the phonon-force oscillations followed the expected behavior. This was particularly visible in the small-field regime where both the spin splitting and the localized states are not very relevant. The pronounced deviations at the highest fields are probably first indications of the development of the fractional quantum Hall effect.

It is interesting to analyze the theoretical magnetic-field dependence of the phonon force in more detail. Equation (21) depends on the magnetic field firstly by the term $l_B D(E_\mu, B)^2$. It follows from Eq. (22) that the first terms of Eq. (21) would not lead to a field dependence of the maximum phonon force. The oscillating behavior of Eq. (21) is, of course, caused by $D(E_\mu, B)$. Secondly, the term $\langle i \mid e^{i\mathbf{q}_s\cdot\mathbf{r}} \mid f\rangle$ contains the magnetic form factor $\exp(-\zeta^2/4)$, which increases with the magnetic field as long as $l_B q_\parallel > 1$ holds. This leads to the increase of the maximum amplitude of the phonon force observed in Fig. 6 (bottom). Eventually the form factor given by the thickness of the 2DEG, Eq. (6), becomes more effective. For our experimental situation (phonons propagating in the [012] direction) this is the case if $l_B\sqrt{2} < a_0$ or at about 12 T. This is about the highest magnetic field which was used in the experiments.

VI. CONCLUSION

We have studied the interaction of acoustic phonons with frequencies in the 100-GHz range with a 2DEG at a GaAs/Al$_x$Ga$_{1-x}$As interface using the phonon-drag effect and the phonon-imaging technique. The interaction was theoretically described using a free-electron approach with broadened Landau levels. Screening effects were not considered. The macroscopic response of the 2DEG samples was modeled by assuming that the phonon-drag induces currents in the same way as electric fields.

At zero magnetic field the theoretically expected behavior was reproduced with greater precision than before because the thermoelectric effects were put under control using a 2DEG geometry where the contacts were sufficiently far away from the phonon-sensitive area. The shape of the patterns in the images was not dependent on laser power which means that the $2k_F$ cutoff was not significant. It followed from theory that this is expected

for 10-nm-thick 2DEG where the form-factor cutoff due to the thickness is more effective.

In magnetic fields we could separate the phonon-drag effect from the Nernst-Ettinghausen effect by using the phonon-focusing pattern of the first one. The phonon-drag images looked qualitatively the same as in the zero magnetic field, except for the rotation by 90°, because the relevant part of the interaction matrix elements do not depend on the magnetic field. The field dependence enters by the different cutoff mechanisms which are not easily observed by the heat-pulse technique. The Nernst-Ettinghausen voltages differed qualitatively from the ballistic ones. The whole sample was sensitive to it. Its intensity seemed to be proportional to the derivative of the density of states.

The intensity of the phonon-drag signal, however, oscillated with the density of the extended states at the Fermi edge. It was completely zero if the Fermi energy was in the range of the localized states. It is interesting to note that Esslinger *et al.*[28] found considerable drag voltages and currents in this situation by using coherent surface-acoustic waves in the upper MHz range.

One can now go one step further and invert the theoretical procedure and calculate the DOS from our data. The result is shown in Fig. 7. Thus the phonon-absorption measurements provide another possibility to probe the DOS in addition to capacitance and transport measurement. The problem of the phonon technique, however, is the same problem as in other procedures in that it does not yield the ratio of the localized and extended states directly.

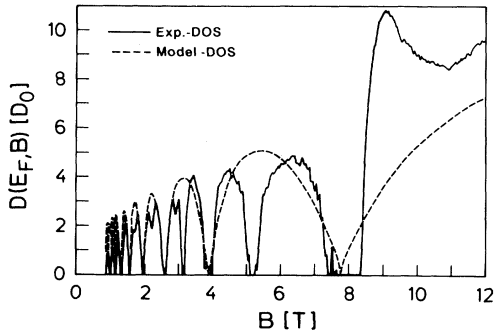

FIG. 7. Density of electronic states extracted from our data in comparison with a model density of states.

ACKNOWLEDGMENTS

We profited greatly from discussions with and support from L.J. Challis, V.I. Fal'ko, A.J. Kent, K.v. Klitzing, R. Knott, R. Nötzel, and R. Wichard. This work was partly supported by the SCIENCE program of the European Community.

*Present address: Lahmeyer International GmbH, W-6000 Frankfurt 21, Germany.

[1] J. C. Hensel, R. C. Dynes, and D. C. Tsui, Phys. Rev. B **28**, 1124 (1983).
[2] M. Rothenfusser, L. Köster, and W. Dietsche, Phys. Rev. B **34**, 5518 (1986).
[3] J. P. Eisenstein, V. Narayanamurti, H. L. Stormer, A. Y. Cho, and J. C. M. Hwang, in *Phonon Scattering in Condensed Matter V*, edited by A. C. Anderson and J. P. Wolfe (Springer, Berlin, 1986), p. 401.
[4] A. J. Kent, G. A. Hardy, P. Hawker, V. W. Rampton, M. I. Newton, P. A. Russell, and L. J. Challis, Phys. Rev. Lett. **61**, 180 (1988).
[5] H. Karl, W. Dietsche, A. Fischer, and K. Ploog, Phys. Rev. Lett. **61**, 2360 (1988).
[6] J. P. Eisenstein, A. C. Gossard, and V. Narayanamurti, Phys. Rev. Lett. **59**, 1341 (1987).
[7] A. Lega, H. Karl, W. Dietsche, A. Fischer, and K. Ploog, Surf. Sci. **229**, 116 (1990).
[8] G. A. Toombs, F. W. Sheard, D. Neilson, and L. J. Challis, Solid State Commun. **64**, 577 (1987).
[9] S. Tamura and H. Kitagawa, Phys. Rev. B **40**, 8485 (1989).
[10] R. Fletcher, J. C. Maan, K. Ploog, and G. Weimann, Phys. Rev. B **33**, 7122 (1986).
[11] C. Ruf, H. Obloh, B. Junge, E. Gmelin, K. Ploog, and G. Weimann, Phys. Rev. B **37**, 6377 (1988).
[12] B. K. Ridley, *Quantum Processes in Semiconductors* (Oxford University Press, Oxford, 1988).
[13] F. Dietzel, Dissertation, Universität Stuttgart, 1992.
[14] S. S. Kubakaddi, P. N. Butcher, and B. G. Mulimani, Phys. Rev. B **40**, 1377 (1989).
[15] S. K. Lyo, Phys. Rev. B **40**, 6458 (1989).
[16] T. M. Fromhold, P. N. Butcher, G. Qin, B. G. Mulimani, J. P. Oxley, and B. L. Gallagher, Surf. Sci. **263**, 183 (1992).
[17] V. I. Fal'ko and S. V. Iordanskii, J. Phys. Condensed Matter **4**, 9201 (1992).
[18] A. L. Efros and Yu. M. Galperin, Phys. Rev. Lett. **64**, 1959 (1990).
[19] A. J. Kent, D. J. McKitterick, L. J. Challis, P. Hawker, and C. J. Mellor, Phys. Rev. Lett. **69**, 1684 (1992).
[20] V. Narayanamurti, R. A. Logan, and M. A. Chin, Phys. Rev. Lett. **40**, 63 (1978).
[21] E. F. Schubert, K. Ploog, H. Dämbkes, and K. Heime, Appl. Phys. A **33**, 63 (1984).
[22] G. A. Northrop and J. P. Wolfe, Phys. Rev. Lett. **43**, 1424 (1979).
[23] F. Rösch and O. Weis, Z. Phys. B **46**, 33 (1977).
[24] F. Dietzel, W. Dietsche, and K. Ploog, Physica B **165&166**, 877 (1991).
[25] Cz. Jasiukiewicz, D. Lehmann, and T. Paszkiewicz, Z. Phys. B **86**, 225 (1992).
[26] T. Ando, A. B. Fowler, and F. Stern, Rev. Mod. Phys. **54**, 437 (1982).
[27] M. Neuberger, *III-V–Semiconducting Compounds* (Plenum, New York, 1971), p. 45.
[28] A. Esslinger, A. Wixforth, R. W. Winkler, J. P. Kotthaus, H. Nickel, W. Schlapp, and R. Lösch, Solid State Commun. **84**, 939 (1992).

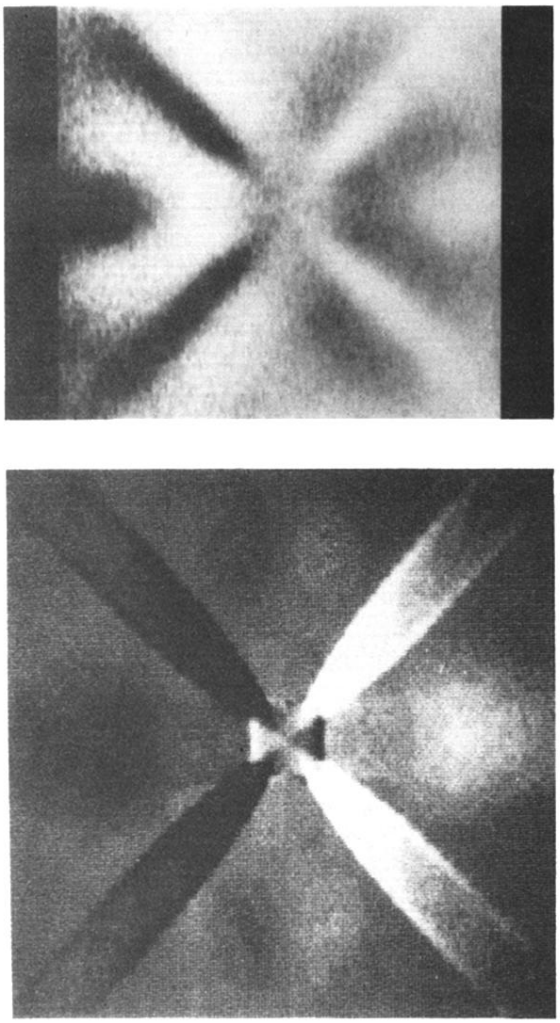

FIG. 2. Top: Image of the phonon-drag voltage in zero magnetic field measured using the contacts 2/5 of Fig. 1. An average gray tone corresponds to zero signal. Positive and negative signals are represented as dark and bright shades, respectively. The sharp diagonal ridges are due to FTA phonons while the round areas in the left and right are caused by LA phonons traveling near the $\langle 111 \rangle$ directions. Bottom: Phonon-drag image calculated using the piezoelectric interaction.

FIG. 3. Image of the phonon-induced voltages across the contacts 2/3 in a magnetic field of about 4.5 T. The Fermi energy is in the lower half of a Landau level. The large diffuse areas (bright at top, dark at bottom) are due to the Nernst-Ettinghausen effect. A ballistic phonon-drag image is superimposed on this image but is hardly visible in the reproduction.

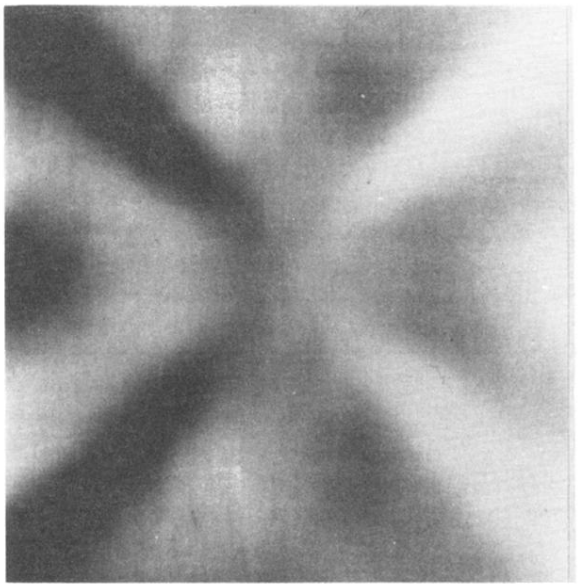

FIG. 4. Ballistic phonon-drag image taken at $B \approx 12$ T by measuring the voltages across the contacts 2/3. At this field the Nernst-Ettinghausen effect was zero because the Fermi energy was in the center of a Landau level. Note that the image is not rotated with respect to the image of Fig. 1.